# Complexation Mechanism of Bovine Serum Albumin and Poly(allylamine hydrochloride)

**V. Ball,*,† M. Winterhalter,‡ P. Schwinte,§ Ph. Lavalle,§ J.-C. Voegel,§ and P. Schaaf†**

*Institut Charles Sadron, Centre National de la Recherche Scientifique, Unité Propre 22, 6 rue Boussingault, 67083 Strasbourg Cedex, France, Institut de Pharmacologie et de Biologie Structurale, Centre National de la Recherche Scientifique, Unité mixte de recherche 5089, 205 route de Narbonne, 31077 Toulouse, France, and Faculté de Médecine, Institut National de la Santé et de la Recherche Médicale, Unité 424, 11 rue Humann, 67085 Strasbourg Cedex, France*

*Received: July 3, 2001; In Final Form: November 19, 2001*

The mechanism of aggregation of bovine serum albumin (BSA) by poly(allylamine) hydrochloride (PAH) is investigated as a function of the mixing ratio $r$ defined as the ratio of the number of BSA molecules and PAH chains present in the solution, under pH conditions of strong binding between the two partners. It is found that as $r$ increases the turbidity first increases, passes through a maximum at a value $r_{max}$ before decreasing again. For small and large values of $r$, one forms small aggregates in the 10 nanometer size range, whereas at $r_{max}$, the size of the aggregates becomes of the order of micrometers. The structure of the aggregates appears to be independent of the history of the systems but depends only on the value of $r$ despite the strong BSA/PAH binding. The desaggregation of the large aggregates formed at $r_{max}$ by the addition of BSA or PAH is shown to be an isenthalpic process and is thus entirely entropically driven. Moreover, we prove that $r_{max}$ corresponds to the state of the system where both the PAH chains and the BSA molecules interact one with each other, both with their maximum number of interaction points per molecule. This explains the independence of $r_{max}$ on the BSA or PAH concentration in the solution and why it varies linearly with the molecular weight of the polyelectrolyte. Moreover, we show that at $r_{max}$, all the BSA and PAH molecules present in the solution are involved in the aggregates. At small (respectively large) values of $r$, the aggregates appear positively (respectively negatively) charged, corresponding to a charge excess at the surface of the aggregates. Finally, it is found that the protein/polyelectrolyte interaction is endothermic, indicating that the BSA/PAH binding must thus be entropically driven. The binding enthalpy of BSA molecules with PAH chains for $r < r_{max}$ is of the order of 400 kJ·mol$^{-1}$ of BSA molecules for solutions containing less than 0.1M of NaCl. The effect of the salt concentration of the solution on the binding process is also briefly discussed.

## I. Introduction

Proteins can primarily be considered as charged amphoteric colloidal particles. They can thus interact electrostatically with polyelectrolytes, DNA or RNA chains[1,2] forming various structures such as complex coacervates[3,4] or soluble complexes. The studies of the interactions between polyelectrolytes and proteins started already in the 1950s by Morawetz and co-workers.[5,6] They described the precipitation of liver catalase by some synthetic polyelectrolytes. More recently, the interactions between cationic peptides and nucleic acids were extensively investigated focusing mainly on thermodynamic aspects.[1] Dubin and co-workers undertook also systematic investigations of the structural behavior of several protein/polyelectrolyte systems in solution.[7−10] Using a variety of experimental techniques such as turbidimetry or light scattering, they found, by changing gradually the pH, the existence of at least two transition points. There is first a well-defined pH at which binding between the polyelectrolyte chains and the proteins starts. This pH is defined as $pH_{crit}$. It is characterized by a sudden increase in the light scattering, whereas the turbidity of the solution remains small.[10] Light scattering being sensitive to refractive index differences at the length scale of macromolecules, whereas turbidity is more sensitive to large scale refractive index inhomogeneities,[11] this indicates the formation of small soluble complexes at $pH_{crit}$.[12] $pH_{crit}$ depends on the ionic strength of the solution[10] and is often observed in the pH range where the net charge of the protein is of the same sign as the charge of the polyelectrolyte. This is explained by protein charge heterogeneity, the polyelectrolyte interacting with charged patches of opposite sign to that of the average protein charge.[8] Although the pH is further increased, light scattering suddenly increases strongly to reach a maximum at a pH denoted as $pH_{\phi}$. At this point, the turbidity also starts to increase very rapidly before decreasing again for higher pH values. Contrast phase microscopy reveals the formation of droplets at $pH_{\phi}$.[10] The formation of such large structures which are usually described as coacervates,[3] must originate from strong interactions between the polyelectrolytes and the proteins leading to the formation of stable binding. Upon a further increase of the pH, due to the formation of a solid precipitate[10] or the redissolution of the large aggregates, both the light scattering and the turbidity decrease.

Despite this general view of the structural behavior of a protein/polyelectrolyte system in solution, a clear picture of the

* To whom all correspondence should be addressed.Tel: (0033) 3 88 41 40 12. Fax: (0033) 3 88 41 40 99. E-mail: ball@ics.u-strasbg.fr.

† Institut Charles Sadron, Centre National de la Recherche Scientifique.

‡ Institut de Pharmacologie et de Biologie Structurale, Centre National de la Recherche Scientifique.

§ Institut National de la Santé et de la Recherche Médicale.

10.1021/jp012522m CCC: $22.00 
Published on Web 02/09/2002

different physical processes leading to these structural changes at a molecular level is still not available. Interactions between proteins and polyelectrolytes are usually described as being of electrostatic origin. This however is rather vague. Thermodynamic studies of positively charged oligopeptides binding to DNA and RNA have revealed that such electrostatic interactions correspond in fact to an entropy increase resulting from the release of cations previously bound to the nucleic acids.[13−17] For synthetic polyelectrolytes interacting with proteins, it is postulated that the interaction process is the result of a competition between the attractive electrostatic interactions of the polyelectrolytes and the proteins and the loss of polymer conformational entropy as described in Muthukumar's model.[18,19]

To get a better understanding of these systems, we investigated the interactions between poly(allylamine hydrochloride) (PAH) and bovine serum albumin (BSA) at a pH above $pH_\phi$ where the formation of large stable complexes is observed. We focus on the structural evolution of the system as a function of the mixing ratio *r*, defined as the ratio between the number of the protein and the number of PAH molecules in solution. We address special attention to the reversibility of the BSA/PAH aggregation process with respect to changes in *r*. We show that the structure of these aggregates does depend neither on the history of their formation nor on the BSA or PAH concentration but only on the mixing ratio *r*. These systems are thus at thermodynamic equilibrium. Using isothermal microcalorimetry we also determine the interaction enthalpy between PAH and BSA molecules. We find that the net interaction between BSA molecules and PAH chains is endothermic with a $\Delta H$ of interaction that decreases when the ionic strength is increased. These results indicate that the interactions between BSA and PAH responsible for their strong binding and the formation of BSA/PAH complexes are mainly of electrostatic and ultimately of entropic origin. The increase in entropy as the interactions take place can be attributed to the release of the protein and polyelectrolyte counterions, as it was found for DNA or RNA/protein interactions.[14] We also find that for large enough mixing ratios so that all the PAH chains are involved in interactions with BSA molecules, the structural changes of the complexes accompanying an increase of *r* is isenthalpic. Finally, we propose a molecular model for the BSA/PAH complex formation that accounts for all the experimental observations.

## II. Materials and Methods

**Materials.** Bovine Serum Albumin (BSA) was purchased from Sigma ($M_w = 66\,500$ g·mol$^{-1}$, A-7638, lot 79H7614) and used without further purification. Its concentration in solution was measured by optical spectrophotometry (Shimadzu UV-2101 PC) using an extinction coefficient of 0.66 cm$^2$·mg$^{-1}$ at 280 nm.

Most of the experiments were performed with Poly (allylamin hydrochloride) (PAH) ($M_w = 70\,000$ g·mol$^{-1}$, Aldrich, Catalog number 28,322-3 lot 07130MS-030, average degree of polymerization: 1207). Some experiments, in which we studied the effect of the polymer chain length on the BSA/PAH complex formation, were done with PAH of smaller mass ($M_w = 15\,000$ g·mol$^{-1}$, Aldrich, Catalog number, 28,321-5). The polyelectrolyte and the protein were always dissolved in $10^{-2}$ M Tris buffer (Gibco BRL, Catalog number: 15504-020, lot number: 1024727, average degree of polymerization: 259) whose pH was adjusted to $7.4 \pm 0.05$ with concentrated hydrochloric acid (Carlo Erba). The ionic strength of these solutions was adjusted by addition of sodium chloride (R. P. Normapur code 270810.295, lot J278). Tris−HCl buffers with 3 different NaCl concentrations (1 M, 0.1 M, and 0.01 M) were used. We define the mixing ratio *r* of a BSA/PAH solution as the ratio between the number of BSA molecules to the number of PAH chains present in the solution. To define more precisely the contribution of the electrostatic interactions, we also define the charge mixing ratio *r** of a solution as the ratio between the number of charges provided by the BSA molecules and the number of charges provided by the PAH chains present in the solution. Typically, at pH 7.4, a BSA molecule carries about 18 negative charges as obtained from titration curves.[20] Between 0.01 and 1 M NaCl, we expect only small variations in this average number of charges carried by the protein. Indeed, the electrostatic interaction parameter which enters in the evaluation of the $pK_a$ modifications of amino acids[21] decreases from $6 \times 10^{-20}$ to $1.6 \times 10^{-20}$ J when the ionic strength increases from $20 \times 10^{-3}$ M to 1.0 M. At pH 7.4, we also assume that all the amino groups of PAH are charged. Then, the relation between *r** and *r*, for PAH chains of mass 70 000 g·mol$^{-1}$ becomes

$$r^* = r \cdot 18/1200 \tag{1}$$

**Evolution of the Turbidity as a Function of *r*, Binding Curves.** A 10.0 cm$^3$ aliquot of buffered protein solutions was added to 10.0 cm$^3$ of a 0.06 mg·cm$^{-3}$ PAH solution under gentle stirring. The obtained solution was then aged for 15 min at room temperature. Then 2 cm$^3$ was withdrawn for turbidity measurements (at $\lambda = 500$ nm, Shimadzu UV-2101 PC spectrophotometer). This was done with buffer solutions of three different ionic strengths: 0.01, 0.1, or 1.0 M NaCl. For the experiments performed at 0.1 M NaCl, the remaining of the solution was centrifuged for 1 h at $10^4$ rpm (Sigma 3K20 centrifuge) to remove the aggregates. The turbidity of the supernatant as well as its absorbance at 280 nm were then measured, allowing for the evaluation of the amount of BSA molecules which remain present in the supernatant and are thus not involved in the large BSA/PAH complexes. We checked the accuracy of the albumin determination method by performing similar experiments with fluorescein labeled BSA (BSA-FITC, Sigma A-9771, lot 89H7613) for $r = 8$ and $r = 16$. These molecules contained an average of 12 fluorescent labels per protein molecule. The zeta potential of the labeled BSA in the Tris−NaCl buffer at pH 7.4 (Zetasizer 3000 HS) was equal to $-24.1 \pm 1.4$ mV, whereas that of the non labeled BSA was equal to $-20.3 \pm 0.5$ mV. Hence, the electrostatic interactions between the labeled and non labeled protein with the polycation should be very similar. The amount of albumin molecules present in the supernatant was determined by means of fluorescence spectroscopy (Shimadzu RF-450 spectrofluorometer, excitation wavelength between 485 and 495 nm, emission measured at 525 nm). The amount of FITC−BSA bound per unit mass of PAH was in good agreement with the value found by optical spectroscopy. This clearly shows the accuracy of our quantification method based on turbidity and absorbance because contrary to the absorbance value, the intensity of the fluorescence emission is not affected by the light scattered by the small BSA-PAH complexes not removed by centrifugation.

**Viscosity Measurements.** To check if gelation occurs during or after the interactions between BSA and PAH, we measured the viscosity of some of the BSA/PAH solutions using an Oswald type viscosimeter (Viscologic, Sematech, France). The solutions were prepared similarly to the turbidity and binding curve experiments (see above). The experiments were performed at $25 \pm 0.5$ °C.

**Quasi Elastic Light Scattering.** Dynamic light scattering from the initial mixtures as well as from the supernatant obtained

after centrifugation at $10^4$ rpm, were measured at a scattering angle of 90° (Zetasizer 3000 HS, Malvern) and a wavelength of 632.8 nm (He−Ne laser). From the experimentally measured intensity auto-correlation function one determines the scattered intensity distribution versus the hydrodynamic radius of the particles by means of an inverse Laplace transform. We used the software provided by the manufacturer to obtain this distribution. All the presented data result from averaging over 30 runs.

**Electrophoretic Light Scattering.** The electrophoretic mobility was measured in Tris buffer at pH 7.4 in the presence of either 0.01 M or 0.1 M NaCl as a function of $r$ using the electrophoretic light scattering mode of the Zetasizer 3000HS (Malvern). The measurements were performed in conditions of constant current, namely at 5 mA. The principle of electrophoretic mobility measurement applied to protein/polyelectrolyte complexes by means of the Doppler shift of two laser beams interfering at the stationary plane of a rectangular shaped flow cell has been described by others.[7] To calculate the zeta potential from the measured electrophoretic mobility, we used the viscosity of the solution as determined from the previously described viscosity experiments.

**Isothermal Titration Microcalorimetry.** The isothermal titration experiments, in which one can detect heat release or consumption in the $\mu$cal range[22−23] were performed with a Microcal Omega apparatus (Microcal Omega MC-2, Microcal, Northhampton, MA) at a constant temperature of (25 ± 0.5 °C). The reference cell was filled with distilled water. The cells had an internal volume of 1.33 $cm^3$. In each experiment, a constant volume of 2 or 8 $\mu$L of the reactants was injected every 180 s. The injection was done by means of a rotating 250 $\mu$L Hamilton microsyringe ensuring constant stirring of the whole solution at a speed of 400 rpm.

Two kind of experiments were performed. In a series of experiments, we injected a 1 $mg{\cdot}cm^{-3}$ buffered BSA solution in an excess of a 5 $mg{\cdot}cm^{-3}$ buffered PAH solution. Such high concentrations were needed to obtain a good signal-to-noise ratio. The heat of dilution of the proteins was obtained by performing a similar experiment where the PAH solution in the cell was replaced by a pure buffer solution. These kind of microcalorimetry experiments were performed with Tris buffer solutions at pH = 7.4 in the presence of 0.01, 0.1, and 1.0 M NaCl. A second kind of microcalorimetry experiments were conducted in which PAH solutions were injected in BSA solutions until the released or consumed heat became equal to the dilution heat of the PAH solution in pure buffer. The amount of PAH at which this occurs allows a direct estimate of the number of cationic polyelectrolytes needed to bind all the BSA molecules present in the calorimeter cell.

## III. Results and Discussion

**A. Structural and Reversibility Aspects of the Formation of BSA/PAH Aggregates.** One of the goals of the present study was to investigate the formation of BSA/PAH aggregates, and in particular to analyze if the structure of the aggregates is history dependent, under pH conditions where the BSA/PAH interactions are strong, i.e., at a pH lying above $pH_\phi$. We thus first determined $pH_{crit}$ and $pH_\phi$ by means of light scattering and turbidimetry measurements as proposed by Dubin and coworkers.[10] The experiments were performed with BSA/PAH solutions containing 0.1 M NaCl at a mixing ratio $r = 16$. They were conducted both by increasing and decreasing gradually the pH of the solution by addition of drops of concentrated HCl or NaOH solutions. We found in both cases the same values

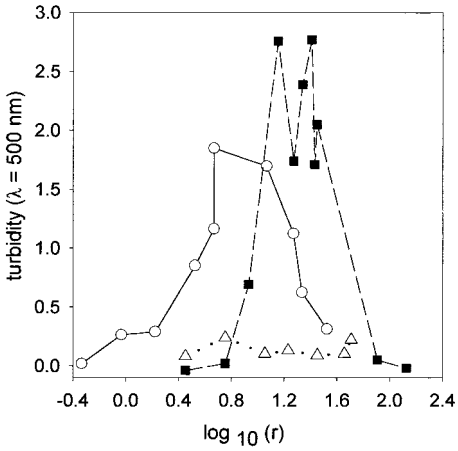


**Figure 1.** Evolution of the turbidity (measured at $\lambda = 500$ nm) as a function of the mixing ratio $r$ at pH 7.4 in a Tris buffer with (■) NaCl 0.01 M, (○) NaCl 0.10 M, and (△) NaCl 1.0 M.

for the turbidity and the intensity of the scattered light, indicating that the BSA/PAH complexation process is reversible with respect to pH changes. For our system, $pH_{crit}$ and $pH_\phi$ are both equal to 4.6 ± 0.2. Taking into account the fact that $pH_{crit}$ is independent of $r$,[10] at least in the dilute polyelectrolyte regime, the critical pH value of 4.6 found for our system is consistent with the value of 4.3 relative to the BSA/PDADMAC (poly(dimethyldiallylammonium chloride)) system reported by Kaibara et al.[10] As expected, the value of 4.6 for $pH_{crit}$ lies below the isoelectric point of BSA which is 4.9.[24] It is, however, surprising that $pH_\phi$ lies also below the isoelectric point of BSA. Indeed, above this pH the protein/polyelectrolyte aggregation process leads to the formation of large stable aggregates, whereas below this pH only small soluble complexes are observed. This pH thus defines the transition from a weak to a strong binding between the protein molecules and the polyelectrolyte chains. All the subsequent experiments were performed at pH = 7.4 under strong binding conditions.

To investigate the reversibility of the formation of BSA/PAH aggregates at pH 7.4 with respect to changes of the mixing ratio $r$ we then studied the structure of the BSA/PAH aggregates as a function of $r$ by mixing directly BSA and PAH solutions at the final proportions. Figure 1 represents the evolution of the turbidity of the BSA/PAH solutions as a function of $r$ obtained under these conditions. In the presence of 0.01 M and 0.1 M NaCl, one observes that the turbidity first increases with $r$ (and $r^*$), passes through a maximum at a value of $r$ that we will denote $r_{max}$ before decreasing again for larger $r$ values. The maximum seems to depend on the ionic strength and is of the order of $r_{max} = 10 \pm 3$ (respectively, $r_{max} = 20 \pm 4$) for an NaCl concentration of 0.1 M (respectively, 0.01 M). This corresponds to values of $r^*$ respectively equal to 0.15 and 0.30. If the same experiments are performed in the presence of 1.0 M NaCl the turbidity remains approximately constant for values of $r$ ranging from 0 to 50. In particular, the turbidity no longer exhibits a maximum. One can notice that all the investigated solutions never display spontaneous sedimentation even over several hours.

To get an idea of the influence of the molecular weight of the polyelectrolyte on the location of the maximum of turbidity with respect to $r$, we performed similar experiments with solutions containing shorter PAH chains ($M_w = 15\,000$ $g{\cdot}mol^{-1}$), at an NaCl concentration of 0.1 M. We find qualitatively the same evolution of the turbidity as a function of $r$ but the maximum is shifted to a value of $r_{max} = 3 \pm 1$ corresponding to a charge mixing ration $r^*$ of 0.21 ± 0.07.

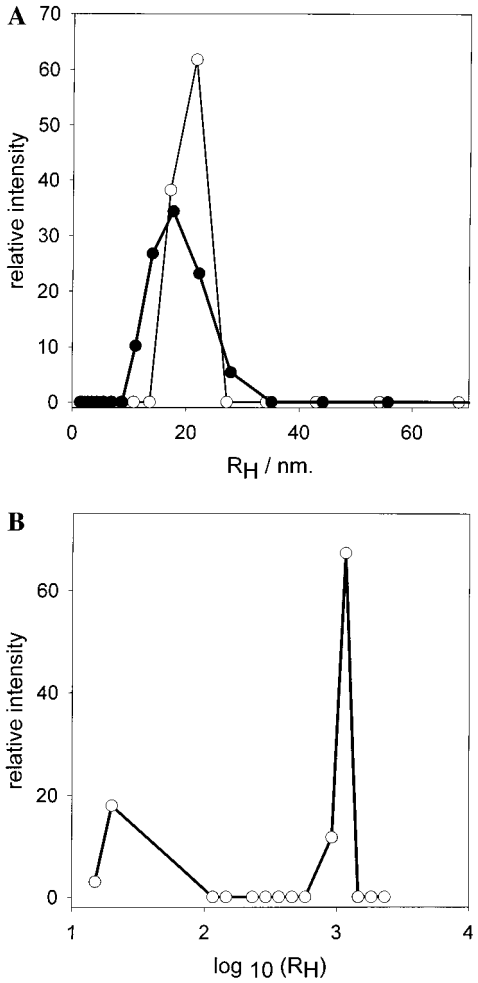


**Figure 2.** (A) Intensity distribution versus the hydrodynamic radius of the particles present in solution for a mixing ratio of 0.33 (○) and 33.3 (●) obtained from light scattering experiments in the Tris−NaCl 0.1 M buffer. The lines do not correspond to a fit but are drawn only to guide the eye. (B) Intensity distribution versus the hydrodynamic radius (logarithmic scale) for a mixing ratio of 10.7 (○), after 50-fold dilution of the initial mixture.

This seems to indicate that, at a given pH, the turbidity maximum is found for a given charge ratio $r^*$ independent of the mass of the polyelectrolyte.

To get an estimate of the size of the aggregates present in the solutions we performed quasi elastic light scattering experiments. Here, we give only a detailed description of the evolution of the size of the aggregates with $r$ for the solutions containing 0.1 M NaCl. Prior to these experiments, to be able to extract from the light scattering experiments the hydrodynamic radii of the particles, we verified that the viscosity of these solutions does not change significantly in the region of large variations of the turbidity. We found that the ratio $\eta_s/\eta_0$ of the viscosity of the solution relative to the viscosity in the absence of proteins and polyelectrolytes varies between 1.02 and 1.1 for $r$ varying between $10^{-1}$ and $10^2$. This indicates in particular that the maximum of turbidity does not correspond to the formation of a gel but is rather the result of the formation of large aggregates as reported for other systems.[7,10] We thus used the viscosities of the pure buffer in order to analyze the light scattering experiments.

For high ($r = 33$) and low ($r = 0.3$) mixing ratios, the analysis of the auto-correlation function of the scattered light shows the presence of a relatively monodisperse distribution of particles with diameters of the order of 15−20 nm (Figure 2A). For low mixing ratios, when PAH is in large excess compared to BSA this must correspond to BSA molecules "decorated" by PAH chains. On the other hand, for high mixing ratios, when the BSA molecules are in large excess compared to PAH these particles must correspond to individual PAH chains "decorated" by BSA molecules. At mixing ratios close to $r_{max}$ the interpretation of the obtained auto-correlation function is not possible due to strong multiple scattering for the BSA and PAH concentrations used in this study. Hence, we diluted the solution with pure buffer in order to obtain the size distribution (Figure 2B). Such a dilution should not influence the particle size distribution which is only a function of $r$ at a given pH and not of the absolute concentrations of BSA and PAH as reported by Kaibara et al.[10] This was confirmed by measuring the turbidity of different solutions obtained by cascade dilution in pure buffer and which are thus all characterized by the same value of $r$ ($r \approx 10$). We found that the turbidity decreases linearly with the dilution ratio of the initial solution (data not shown). Figure 2B shows the presence of two populations of particles: a first population with a characteristic diameter of the order of 20 nm and a population of very large aggregates with a characteristic size of the order of the micrometer. AFM microscopy of a mica surface precoated with PAH and that was brought in contact with such a solution of aggregates confirmed the existence of a population of particles in the micrometer size range together with much smaller particles with a characteristic size lying in the nanometer range, adsorbed on the surface (data not shown).

Qualitatively, a similar particle size evolution as a function of $r$ was found when the experiments were conducted with solutions containing 0.01 M NaCl instead of 0.1 M. However, at large $r$ value, we found in addition to the population with an average radius of about 20 nm, a significant population (about the same contribution as the population of 20 nm in hydrodynamic radius) of particles whose hydrodynamic radii lie in the range between 30 and 45 nm. On the other hand, when the solution contained 1.0 M NaCl, we did not found large aggregates in the micrometer range. Instead, we found that the average hydrodynamic radius of the particles increases monotonically from 105 nm for $r = 5.7$ to 200 nm for $r = 51$. This clearly shows the presence of BSA/PAH aggregates despite the small values of the turbidity. The absence of large aggregates for a given value of $r$ also explains that at this high NaCl concentration one does not observe a turbidity peak. Similar results were reported in the literature for other protein/polyelectrolyte systems.[10]

Electrophoretic light scattering experiments were performed on these solutions in order to get an idea about the variations of the charges of the complexes as a function of the mixing ratio $r$, in particular around the turbidity maximum. Due to the fact that the solution is not composed of an homogeneous population of particles, the zeta potential that is measured is a mean value over the zeta potentials of the particles with a weighting factor that is proportional to the intensity of the light scattered by the different particles. The results are represented in Figure 3. One observes that at low (respectively high) values of $r$ the zeta potential is close to the value measured for a pure PAH (respectively BSA) solution. On the other hand, it becomes zero at $r = r_{max}$ where the maximum of turbidity and the largest aggregates are observed. It thus comes out that the large clusters formed at $r_{max}$ appear as uncharged. This is surprising because $r_{max}$ corresponds to a charge ratio $r^*$ of the order of 0.15 and 0.3 for aggregates formed in solutions containing respectively 0.1 and 0.01 M of NaCl. This means that these large aggregates must contain large amounts of counterions that neutralize their

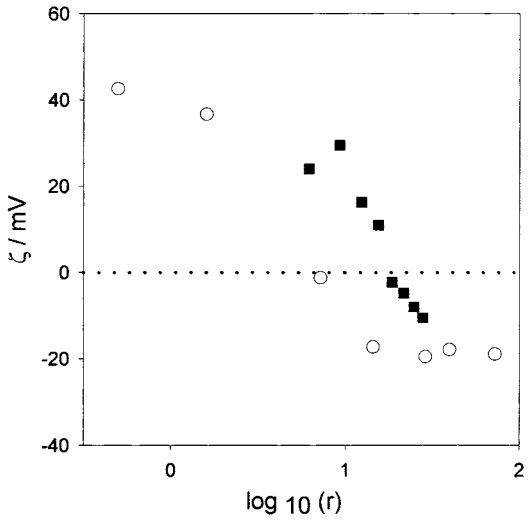


**Figure 3.** Evolution of the zeta potential for the BSA−PAH mixtures as a function of the mixing ratio (in a logarithmic scale) at 0.1 M in NaCl (○) and at 0.01 M in NaCl (■).

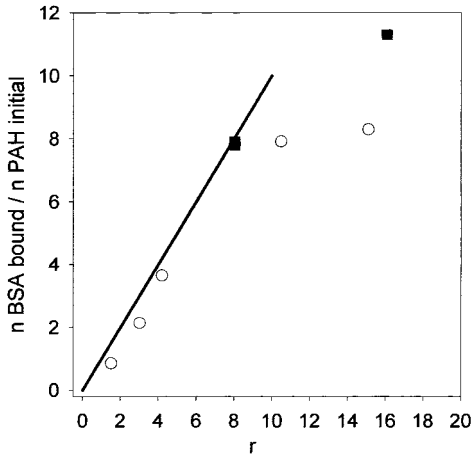


**Figure 4.** Evolution of the number of bound BSA molecules per PAH molecule as a function of the mixing ratio as obtained by depletion measurements after centrifugation by means of UV spectroscopy and light scattering (○). The straight line of slope 1 clearly shows that in the presence of a large excess in PAH, almost all proteins are removed from the bulk. (■) Data obtained with FITC labeled BSA molecules and fluorescence measurements.

net charge. Moreover, the surface of the aggregates must also appear neutral, whereas for mixing ratios different from $r_{max}$ they must exhibit a net charge of similar sign as the one carried by the molecules present in excess in the solution. There seems thus to exist a charge excess on the surface of the aggregates when one of the type of molecules is in excess in the solution. This is similar to what is observed during the buildup of polyelectrolyte multilayers where, polyanions and polycations are adsorbed sequentially on a surface, the buildup driving force after each deposition step being the charge overcompensation created by the polyelectrolyte present in excess in the solution.[25]

We also tried to estimate the amount of unbound proteins that remain free in the solutions. This is an indication of the strength of the protein/polyelectrolyte interaction. Because we never observed a spontaneous sedimentation in these solutions, even after hours, it was necessary to centrifuge them. We assume that the sedimentation consecutive to centrifugation does not affect the fraction of unbound versus bound BSA molecules. Measurements of the optical density at 280 and 500 nm of the supernatants obtained after centrifugation yield the binding curve which represents the average number of bound protein molecules per polyelectrolyte initially present in the solution as a function of the initial mixing ratio. In these experiments, the concentration of PAH is kept fixed (at 0.03 mg·cm$^{-3}$) and the ratio $r$ is varied by changing the initial concentration of BSA in the solution, the NaCl concentration was always 0.1 M. One observes in Figure 4 that at low $r$ values, where the polyelectrolyte is in excess, the slope of the binding curve is equal to one. This indicates that the protein is almost completely removed from the bulk of the solution after centrifugation. BSA appears thus to be completely bound to BSA/PAH complexes. This observation is confirmed with FITC labeled BSA and the measurement of the supernatant fluorescence (Figure 4). The binding curve starts to deviate from the "total binding" line at $r \approx 10$. At higher mixing ratios, the complexes present in the solution were more difficult to remove by centrifugation and the binding curve could thus not be determined precisely. This is confirmed by light scattering experiments of the supernatant, which shows the presence of aggregates in the range of 15−50 nm in radius, whereas for $r$ values smaller than 20 the supernatant of the solutions was free of such aggregates. It indicates that at low $r$ values, the BSA/PAH complexes are probably denser than those obtained at high $r$. We thus represent the binding curve only up to $r = 20$. One can observe that as soon as $r$ exceeds 10, corresponding to $r_{max}$, the number of bound BSA molecules becomes smaller than the number of BSA molecules introduced in the solution and a kind of "saturation" in the number of bound BSA molecules is rapidly reached. The fact that, up to $r = 10$, all the BSA molecules present in the solution are bound to PAH chains is the sign of a strong interaction between the PAH chains and the BSA molecules.

We then investigated the reversibility of the BSA/PAH aggregation process by varying the mixing ratio $r$ at constant pH. Both turbidimetry and quasi elastic light scattering experiments were performed. All the solutions used for this study contained 0.1 M NaCl. We first started with BSA/PAH solutions at a mixing ratio close to 10 corresponding to the maximum of turbidity. Then, we either added a BSA or PAH solution in order to respectively increase or decrease $r$ to a value of 32 or 0.26. The turbidity decreases, whereas $r$ changes. After 2−3 min, it reaches a constant value. The final turbidities are respectively equal to 0.5 and 0.02, values that are similar to the turbidities measured by preparing directly the solutions at their final $r$ values (Figure 1). Figure 5 shows the evolution of the hydrodynamic radii of the particles obtained by light scattering when $r$ was increased from 10 to 32. One observes a strong reduction in the particle size which becomes similar to that measured on a solution prepared directly at the final value of $r = 33$. A similar result is obtained if $r$ is decreased by addition of PAH. This proves that the structure of the aggregates in the solution does not depend on the way in which the solutions are prepared. These systems thus reach thermodynamic equilibrium.

**B. Isothermal Microcalorimetry Experiments.** To get a better understanding of the nature of the BSA/PAH interactions, we performed isothermal microcalorimetry experiments. In these experiments one measures the variation of enthalpy consecutive to the injection of a solute into a solution. If the solution contains only molecules that do not bind to the solute, this enthalpy $\Delta H_{dil}$ corresponds to that of the dilution process of the solute. On the other hand, if molecules from the solution bind with the solute, the measured heat is composed of both the enthalpy of dilution and the enthalpy associated with the binding process itself, $\Delta H_{bind}$. To extract this second component we first determined the heat of dilution of the polyelectrolyte and of the BSA alone.

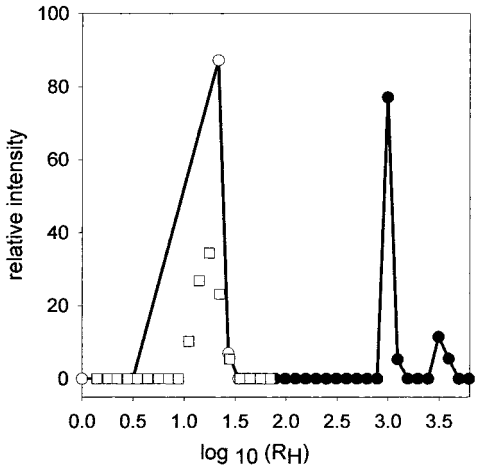


**Figure 5.** Intensity distribution versus the hydrodynamic radius (logarithmic scale) obtained after addition of BSA to a solution containing BSA/PAH aggregates ($r = 15.1$) to reach a final $r$ value of 32 (○) and intensity distribution before addition of BSA (●). These experiments were performed in Tris−NaCl 0.1 M buffer. (□) Intensity distribution obtained by directly mixing BSA and PAH to reach $r = 33.3$ (also shown in Figure 2A). The lines do not correspond to a fit but are drawn to guide the eye.

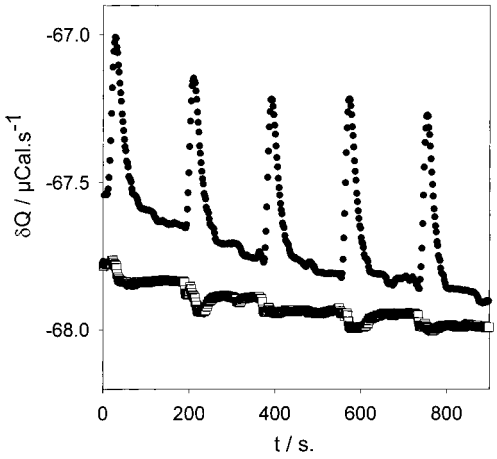


**Figure 6.** Evolution of the heat consumed during successive BSA injections (●) (1.3 mg·cm$^{-3}$, 8 $\mu$L per injection) in a 5.05 mg·cm$^{-3}$ PAH solution in Tris−NaCl 0.1 M buffer. The $r$ value reached at the end of the last injection was equal to $8 \times 10^{-3}$. Heat of BSA dilution in the buffer in the absence of PAH (□). For clarity, this curve is shifted downward with respect to that of the experiment in which BSA is injected in the PAH solution.

These experiments were performed in the same buffer as the one used during mixing of the two solutions. We have found that the enthalpy associated with the dilution of BSA is negligible, less than $-20$ kJ·mol$^{-1}$ (Figure 6) for solutions containing 0.1 M NaCl. On the other hand, the dilution of PAH in pure buffer is a strongly endothermic process (data not shown). It appears also that the dilution enthalpy of PAH strongly decreases when the ionic strength of the solution is increased.

In a first series of experiments, to avoid the important contribution of the dilution of PAH, the microcalorimetry experiments were performed by introducing a small volume of a concentrated BSA solution in a large volume of a PAH solution. Figure 6 represents the evolution of the amount of energy in the form of heat that has been supplied to the system in order to maintain the temperature within the cell equal to the temperature in the reference cell. Due to the fact that the dilution enthalpy of BSA is small, this heat is almost entirely

**TABLE 1: Evolution of the Binding Enthalpy between BSA and PAH as a Function of the Ionic Strength at pH 7.4**

| $C_{NaCl}$/mol·L$^{-1}$ | $\Delta H_{binding}$/kJ·mol$^{-1}$ |
|---|---|
| 0.01 | 390 ± 60 |
| 0.1 | 425 ± 40 |
| 1 | 87 ± 45 |

associated with the binding enthalpy of albumin with PAH. One observes that the enthalpy associated with the BSA/PAH interaction is positive indicating that the binding process is endothermic. The binding enthalpy of BSA to an excess of PAH is given in Table 1 for the three NaCl concentrations that were explored. Although it is of the order of $+400$ kJ·mol$^{-1}$ of BSA molecules for solutions containing 0.1 M and 0.01 M of NaCl, it becomes much smaller when the NaCl concentration is 1.0 M. These values are independent of the BSA concentration of the solution introduced into the PAH solution as long as the mixing ratio $r$ reached at this stage of the titration remains smaller than $r_{max}$. This confirms that, for low $r$ values ($r < r_{max}$) all the BSA molecules are bound to PAH chains and certainly interact with PAH chains through multiple points. The fact that the binding of BSA to PAH is an endothermic process proves that the binding process must be entropically driven. The smaller value of $\Delta H_{bind}$ found with 1.0 M NaCl can be due to the fact that at this high salt concentration the mean number of interactions between a BSA molecule, and the PAH chains in excess is much smaller than for smaller salt concentrations. It could also originate from the fact that the interactions between PAH and BSA are weaker. Both reasons together may ultimately be at the origin of the strong decrease of $\Delta H_{bind}$ at high NaCl concentrations.

We also performed microcalorimetry experiments in which we started from a solution at a mixing ratio close to $r_{max}$ and added BSA molecules to reach a $r$ value close to 40. These experiments were performed in the presence of 0.1 M NaCl. We did not find any heat release or consumption during this process (data not shown). This shows that the number of BSA/PAH interaction points does no longer increase after the value of $r_{max}$ has been reached.

We performed also a second kind of microcalorimetry experiments in which PAH solutions were injected in the BSA solution. These experiments were only conducted with solutions containing 0.1 M of NaCl. These injections were done up to the point where the heat consumption following a PAH solution injection became equal to $\Delta H_{dil}$ of the PAH solution in pure buffer.

Figure 7 shows the evolution of the sum $\sum \Delta H_{bind}$ of the $\Delta H_{bind}$ corresponding to each PAH injection in the BSA solution as a function of the inverse of the mixing ratio of the solution at the end of that injection, i.e., as a function of the number of PAH chains present in the solution, the number of BSA molecules in the solution remaining fixed. As expected from the first type of microcalorimetry experiments the binding enthalpy is positive, showing that the process is endothermic. Moreover, the value of $\sum \Delta H_{bind}$ first increases roughly linearly with $1/r$ before saturating (Figure 7). The value of $r$ where the saturation takes place is, within experimental errors, equal to $r_{max}$ and $\sum \Delta H_{bind}$ in the plateau is equal to $390 \pm 80$ kJ·mol$^{-1}$ of BSA molecules present in the solution. This value is very close to the value of $\Delta H_{bind}$ found when small amounts of BSA molecules were injected in a PAH solution. The existence of this plateau also shows that the addition of PAH chains to a solution at $r_{max}$ is isenthalpic. This, together with the fact that

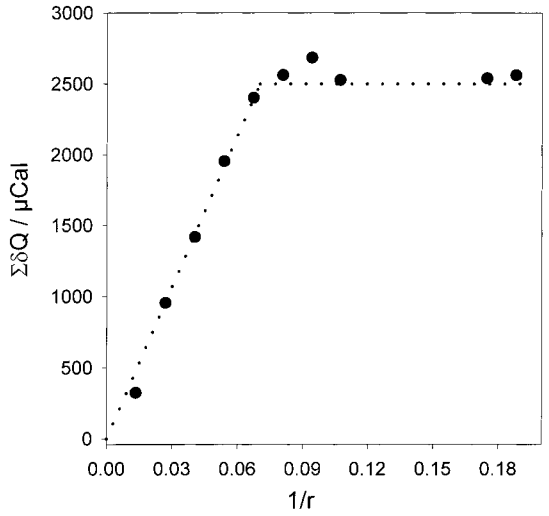


**Figure 7.** Sum of the binding enthalpies calculated (after subtraction of the dilution heat) from a microcalorimetry experiment in which PAH (5.05 mg·cm$^{-3}$) was injected in the calorimeter cell containing BSA (1.34 mg·cm$^{-3}$). The ascending straight line corresponds to the regular enthalpy increment associated with the BSA−PAH interaction as long as some free BSA remains in solution. The horizontal straight line (after $1/r = 0.08$) means that all the initially present BSA is bound to the PAH and that all further PAH addition in the cell does not induce any further heat uptake or release as that associated with its dilution heat in the Tris buffer with 0.1 M NaCl.

the addition of BSA molecules to a solution at $r_{max}$ is also an isenthalpic process, proves that $r_{max}$ corresponds to the mixing ratio where both the BSA and the PAH molecules interact through their maximum possible number of interaction points per molecules. This explains why $r_{max}$ is independent of the concentrations of BSA or PAH. It also shows that the desaggregation of the large BSA/PAH complexes formed at $r_{max}$ by addition of BSA or PAH is entropically driven.

The binding of proteins to polyelectrolytes must be associated with a loss of chain conformational entropy. On the other hand such a binding process corresponds to a release of counterions from the protein and the polyelectrolyte charges during the formation of charge/charge interactions between the two macromolecules. During such a process, the loss of configurational entropy of the chains must be overcompensated by a gain of entropy associated with the release of the counterions. The enthalpy associated with this process should be positive, the counterions being able to come in closer contact with the polyelectrolyte and protein charged groups than do the protein charges with the polyelectrolyte ones. Such an entropically driven mechanism is also known to govern the interactions between nucleic acids and proteins or oligopeptides.[13−17] It is thus not the direct Coulombic interactions between the positive and negative charges present on the two interacting macromolecules that is responsible for the strong interaction between them but the counterion release associated with the process. This could also constitute the driving force for the buildup process of polyelectrolyte multilayers. This explanation should also hold for other polyelectrolyte/protein systems where a similar behavior is observed and it could even be valid for all the electrostatically driven macromolecule/macromolecule interactions.

**C. Molecular Picture of the BSA/PAH Aggregation Process.** All these results lead to the following molecular picture for the aggregation process of BSA interacting with PAH: at low mixing ratios all the BSA molecules interact with PAH chains through multiple points, one BSA molecule certainly interacting with several PAH chains. The probability that PAH chains form bridging between BSA molecules is small due to the large excess of PAH chains in the solution when compared to the BSA molecules. The BSA/PAH complexes are thus of small size and one should find an excess of PAH chains at the outer surface of the aggregates. This explains the value of the zeta potential of the aggregates at small $r$ values. When the mixing ratio and, hence, the protein concentration, increases, the probability that a single PAH chain interacts with several BSA molecules (bridging) increases, leading to BSA/PAH complexes of larger size. Our results suggest that by increasing $r$ ($r < r_{max}$), the total number of interaction points that a BSA molecule creates with all the PAH chains present in the solution remains constant and equal to its maximum possible number. In the meanwhile, the mean number of interaction points that a PAH chain establishes with the BSA molecules increases. When this number attains its maximum value, one reaches $r_{max}$, a point where the size of the BSA/PAH aggregates is maximum giving rise to a maximum in turbidity. We have shown that at this point all the BSA and PAH molecules present in the solution are involved in aggregates. Because none of the two molecules, BSA or PAH, is in excess, there is also no excess of one of the two molecules on the surface of the aggregates which shows up by the fact that their zeta potential is zero. If one further adds BSA molecules in this solution so that the BSA molecules are in large excess compared to the PAH chains (high values of $r$), a given PAH chain creates multiple links with different BSA molecules present in solution, the probability for one BSA molecule to be in contact with two PAH chains becoming extremely small. The BSA/PAH complexes are thus again of small size with an excess of BSA molecules on their surfaces. The fact that an increase (or decrease) of $r$ from $r_{max}$ to higher (lower) values by addition of BSA (PAH) is an isenthalpic process comes from the fact that the structural changes accompanying these molecule additions take place at a fixed number of total interactions between the BSA and PAH molecules present in the solution.

## IV. Summary

In this paper, we investigated the mechanism of BSA/PAH aggregation as a function of the mixing ratio in pH conditions of strong binding between the two partners. One finds that as $r$ increases the turbidity first increases, passes through a maximum at a value $r_{max}$ before decreasing again. For small and large values of $r$ one forms small aggregates in the 10 nanometer size range, whereas at $r_{max}$, the size of the aggregates can become of the order of micrometers. We have shown that the structure of the aggregates is history independent and depends only on the value of $r$ despite the strong BSA/PAH binding. We proved that the desaggregation of the large aggregates formed at $r_{max}$ by the addition of BSA or PAH to a solution at $r_{max}$ is an isenthalpic process and is thus entirely entropically driven. Moreover, we could prove that $r_{max}$ corresponds to the state where all the PAH chains and all the BSA molecules are involved in aggregates, both with their maximum number of interaction points per molecule. This explains why $r_{max}$ does not depend on the BSA or PAH concentration in the solution and varies linearly with the mass of the polyelectrolyte. This is also at the origin of the zero zeta potential of the aggregates at $r_{max}$. Finally, we showed that the protein/polyelectrolyte interaction is endothermic so that the binding must be entropically driven. We could estimate the binding enthalpy of BSA molecules with PAH chains for $r < r_{max}$ to be of the order of 400 kJ·mol$^{-1}$ of BSA molecules for solutions containing less than 0.1 M of NaCl.

**Acknowledgment.** This work has been done with financial support from INSERM-CNRS Grant "Ingéniérie tissulaire" No. 4G005F.

## References and Notes

(1) Record, M. T., Jr.; Ha, J.-H.; Fisher, M. A. *Methods Enzymol.* **1991**, *208*, 291.
(2) Lohman, T. M.; Mascotti, D. P. *Methods Enzymol.* **1992**, *212*, 400.
(3) Bungenberg De Jong, H. *Crystallisation−Coacervation−Flocculation* In *Colloid Science II*; Kruyt H. R. Editor, Elsevier: 1952.
(4) Piculell, L.; Lindman, B. *Adv. Colloid Interface Sci.* **1992**, *41*, 149.
(5) Morawetz, H.; Hughes, W. L. *J. Phys. Chem.* **1952**, *55*, 64.
(6) Berdick, M.; Morawetz, H. *J. Biol. Chem.* **1954**, *206*, 959.
(7) Xia, J.; Dubin, P. L.; Dautzenberg, H. *Langmuir* **1993**, *9*, 2015.
(8) Hallberg, R. K.; Dubin, P. L. *J. Phys. Chem. B* **1998**, *102*, 8629.
(9) Mattison, K. W.; Dubin, P. L.; Brittain, I. J. *J. Phys. Chem. B* **1998**, *102*, 3830.
(10) Kaibara, K.; Okazaki, T.; Bohidar, H. B.; Dubin, P. L. *Biomacromolecules* **2000**, *1*, 100.
(11) Urwin, J. R. *Molecular Weight Distributions by Turbidimetric Titration* in *Light Scattering from Polymer Solutions*; Huglin, M. B., Ed., Academic Press: 1972, chapter 18.
(12) Dellacherie, E. *Am. Chem. Soc. Div. Polym. Chem. Prepr.* **1991**, *32*, 602.
(13) Record, M. T., Jr.; Lohman, T. M.; Haseth, P. L. *J. Mol. Biol.* **1976**, *107*, 145.
(14) Mascotti, D. P.; Lohman, T. M. *Proc. Natl. Acad. Sci. U.S.A.* **1990**, *87*, 3142.
(15) Mascotti, D. P.; Lohman, T. M. *Biochem.* **1992**, *31*, 8932.
(16) Mascotti, D. P.; Lohman, T. M. *Biochem.* **1993**, *32*, 10568.
(17) Mascotti, D. P.; Lohman, T. M. *Biochem.* **1997**, *36*, 7272.
(18) Muthukumar, M. *J. Chem. Phys.* **1987**, *86*, 7230.
(19) Muthukumar, M. *J. Chem. Phys.* **1995**, *103*, 4723.
(20) Tanford, C. *J. Am. Chem. Soc.* **1950**, *72*, 441.
(21) Linderström-Lang, K. *Compt. Rend. Trav. Lab. Carlsberg* **1924**, *15*, 7.
(22) Seelig, J. *Biochim. Biophys. Acta* **1997**, *1331*, 103.
(23) Jelesarov, I.; Bosshard, H. R. *J. Mol. Recognit.* **1999**, *12*, 3.
(24) Peters, J. T. *Adv. Protein Chem.* **1985**, *33*, 167.
(25) Ladam, G.; Schaad, Ph.; Voegel, J. C., Schaaf, P.; Decher, G.; Cuisinier, F. J. G. *Langmuir* **2000**, *16*, 1249.